Digital Transmission via Underwater Acoustic Particle Velocity Channels

C. Chen[1], A. Abdi[1], A. Song[2], and M. Badiey[2]

1 Center for Wireless Communication and Signal Processing Research
Dept. of Electrical and Computer Engineering, New Jersey Institute of Technology, Newark, NJ 07102, USA

2 Physical Ocean Science and Engineering
College of Earth, Ocean, and Environment, University of Delaware, Newark, DE 19716, USA

Emails: cc224@njit.edu, abdi@adm.njit.edu, ajsong@udel.edu, badiey@udel.edu

***Abstract*—Recent studies have shown that a compact underwater vector sensor receiver can perform as an array of scalar sensors. Here we propose a scheme to transmit data via underwater particle velocity channels using a dipole vector sensor. System equations are derived and simulations are presented. This demonstrates the possibility of digital transmission using a vector sensor.**

I. Introduction

Vector sensors measure the signal not only in the pressure channel, but also in particle velocity channels. In the past few decades, a large volume of research has been conducted on the theory and design of vector sensors, mainly used in SONAR systems and underwater target localization [1] [2] [3] [4], due to the highly directional information that vector sensors provide. Recent achievements in material science and manufacturing technologies provide low noise and small vector sensors with wide dynamic ranges [4] [5]. Recently vector sensors are proposed to be used at the receive side of underwater acoustic communication systems, for multichannel equalization [6] [7]. More specifically, a multichannel receiver is proposed [6] [7] with one pressure sensor as the transmitter and a vector sensor as the receiver. Statistical characteristics of acoustic particle velocity channels are expressed in [8].

Since a vector sensor has a compact size, small platforms such as unmanned underwater vehicles will significantly benefit if a compact vector sensor can be used for signal transmission as well. The key to this problem is to find out how signal can be transmitted via particle velocity channels. A dipole vector sensor is composed of two closely-placed pressure sensors that measure the spatial gradient of the field [5]. So, the spatial gradient between the data on these two pressure sensors can be viewed as the signal which is modulated on the dipole, in the direction of the axis of the dipole. One interpretation could be that the signal is transmitted via a particle velocity channel which is aligned with the direction of the dipole. The key advantage of the proposed dipole transmitter is that in the reverse (reception) mode, it provides diversity.

In this article, a communication system with one dipole at the transmitter and a vector sensor at the receiver is proposed. In Section II, the schematic of this system is presented and system equations are derived. System performance analysis and simulation results are provided in Section III, and Section IV concludes the paper.

This work is supported in part by the National Science Foundation (NSF), Grant CCF-0830190

II. Signals and Channels in The Proposed System

In the two-dimensional *y*-*z* (range-depth) plane, a vector sensor device measures three components of the field: acoustic pressure, and *y* and *z* components of the acoustic particle velocity. A pressure sensor in the device measures the acoustic pressure. The *y* and *z* components of particle velocity can be measured by two dipoles in *y* and *z* directions, respectively, by spatial differentiation of the acoustic field in each direction. In Fig. 1 there is one dipole at the transmitter and two dipoles at the receiver. The dipole at the transmitter *Tx* is parallel to the *z* axis and the two pressure sensors in *Tx* are labeled as 1 and 2. At the receiver *Rx*, the two dipoles are parallel to *y* and *z* axes with their centers at the point (y_0, z_0). They measure the *y* and *z* components of the acoustic particle velocity at (y_0, z_0). The four pressure sensors at *Rx* are labeled as 1, 2, 3 and 4. Another pressure sensor labeled as 5 is located at (y_0, z_0), to measure the acoustic pressure component in the vector sensor device. So, there are ten different pressure channels in Fig. 1, where p_{iq} stands for the channel from sensor i at *Tx* to sensor q at *Rx*, $i = 1,2$ and $q = 1,2,3,4,5$.

According to the linearized equation for time-harmonic waves [5], at frequency f_0, for each sensor in *Tx*, there are two particle velocity channels at *Rx*, the vertical and horizontal components of particle velocity at (y_0, z_0). More specifically, for Tx_1 there are $v_z^{Tx_1}$ and $v_y^{Tx_1}$, whereas for Tx_2 we have $v_z^{Tx_2}$ and $v_y^{Tx_2}$. These four channels are given by the following equations, where $L_{Rx} \to 0$

$$\begin{aligned} v_z^{Tx_1} &= -(j\rho_0\omega_0)^{-1}(p_{11} - p_{12})/L_{Rx}, \\ v_z^{Tx_2} &= -(j\rho_0\omega_0)^{-1}(p_{21} - p_{22})/L_{Rx}, \\ v_y^{Tx_1} &= -(j\rho_0\omega_0)^{-1}(p_{13} - p_{14})/L_{Rx}, \\ v_y^{Tx_2} &= -(j\rho_0\omega_0)^{-1}(p_{23} - p_{24})/L_{Rx}. \end{aligned} \tag{1}$$

Here ρ_0 is the density of the fluid, $j^2 = -1$, $\omega_0 = 2\pi f_0$ and L_{Rx} denotes the spacing between the two pressure sensors in each dipole at *Rx*, as shown in Fig. 1. To transmit the symbol s, we modulate s/L_{Tx} and $-s/L_{Tx}$ on Tx_1 and Tx_2, respectively, where L_{Tx} denotes the distance between the two sensors in the dipole at *Tx*. For the average transmit symbol power we choose $\Omega_s = E[2|s|^2/L_{Tx}^2] = 1$, where E is the expectation

operator. This means the average transmit power is 1. Since z velocity is the spatial gradient of the pressure field in the z direction, this transmission scheme means that the symbol s is modulated on the z velocity channel. This can be better understood by writing the equation for the received signal of each pressure sensor at *Rx*

$$r_1 = ((p_{11} - p_{21})/L_{Tx}) \oplus s,\ r_2 = ((p_{12} - p_{22})/L_{Tx}) \oplus s,$$
$$r_3 = ((p_{13} - p_{23})/L_{Tx}) \oplus s,\ r_4 = ((p_{14} - p_{24})/L_{Tx}) \oplus s, \quad (2)$$
$$r = ((p_{15} - p_{25})/L_{Tx}) \oplus s.$$

Here $\oplus$ is the convolution. As shown in Appendix, each channel $(p_{1q} - p_{2q})/L_{Tx}$ in (2), $q = 1, 2, 3, 4, 5$, is similar to a velocity channel with which the symbol s is convolved.

The z and y particle velocity signals at *Rx* are spatial gradients of the received signals r_1, r_2, r_3 and r_4, measured by the two dipoles, as $L_{Rx} \to 0$

$$\eta_z = -(j\rho_0\omega_0)^{-1}(r_1 - r_2)/L_{Rx},$$
$$\eta_y = -(j\rho_0\omega_0)^{-1}(r_3 - r_4)/L_{Rx}. \quad (3)$$

By combining (1), (2) and (3), the z and y velocity components at *Rx* can be written as

$$\eta_z = (v_z^{Tx_1} - v_z^{Tx_2})/L_{Tx} \oplus s,\ \eta_y = (v_y^{Tx_1} - v_y^{Tx_2})/L_{Tx} \oplus s. \quad (4)$$

Now we convert velocity channels and signals to pressure-equivalent quantities. Corresponding to the four particle velocity channels in (1), there are four *pressure-equivalent* particle velocity channels $p_z^{Tx_1}$, $p_z^{Tx_2}$, $p_y^{Tx_1}$, $p_y^{Tx_2}$, obtained by multiplying (1) with the negative of the acoustic impedance $-\rho_0 c$ [6]

$$p_z^{Tx_1} = -\rho_0 c v_z^{Tx_1},\ p_z^{Tx_2} = -\rho_0 c v_z^{Tx_2},$$
$$p_y^{Tx_1} = -\rho_0 c v_y^{Tx_1},\ p_y^{Tx_2} = -\rho_0 c v_y^{Tx_2}. \quad (5)$$

In the above equations, c is the sound speed.

Similarly, the *pressure-equivalent* z and y velocity components at *Rx* are η_z and η_y multiplied by $-\rho_0 c$

$$r_z = -\rho_0 c \eta_z,\ r_y = -\rho_0 c \eta_y. \quad (6)$$

By substituting (4) into (6) and upon using the definitions in (5) we obtain

$$r_z = ((p_z^{Tx_1} - p_z^{Tx_2})/L_{Tx}) \oplus s,$$
$$r_y = ((p_y^{Tx_1} - p_y^{Tx_2})/L_{Tx}) \oplus s. \quad (7)$$

To include the effect of noise, *pressure-equivalent* ambient velocity noise terms n_z and n_y should be added to (7), whereas the ambient pressure noise n needs to be added to the last equation in (2). The final set of noisy signals received at *Rx* is given by

$$r_z = ((p_z^{Tx_1} - p_z^{Tx_2})/L_{Tx}) \oplus s + n_z,$$
$$r_y = ((p_y^{Tx_1} - p_y^{Tx_2})/L_{Tx}) \oplus s + n_y, \quad (8)$$
$$r = ((p_{15} - p_{25})/L_{Tx}) \oplus s + n.$$

As shown in [6], for the isotropic noise model, the noise terms in (8) are uncorrelated, that is $E[n\{n_y\}^*] = E[n\{n_z\}^*] = E[n_z\{n_y\}^*] = 0$. Moreover, for the powers of the noise terms in (8) we have $\Omega_n = E[|n|^2]$ and $\Omega_n^y = E[|n_y|^2] = \Omega_n^z = E[|n_z|^2] = \Omega_n/2$.

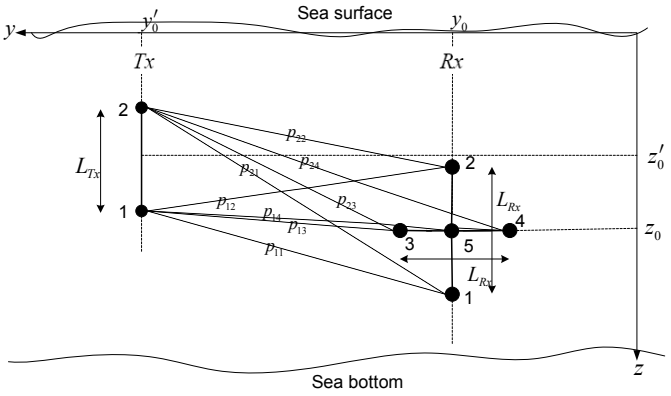

Fig. 1. The proposed vector sensor underwater acoustic communication system.

III. System Performance and Simulation Results

Let $\tilde{\mathbf{p}}_d = [\tilde{p}_d(0) \ldots \tilde{p}_d(M-1)]^T$, $\tilde{\mathbf{p}}_d^y = [\tilde{p}_d^y(0) \ldots \tilde{p}_d^y(M-1)]^T$ and $\tilde{\mathbf{p}}_d^z = [\tilde{p}_d^z(0) \ldots \tilde{p}_d^z(M-1)]^T$, with ^{T} as transpose, be the taps of the three channel impulse responses in (8), such that $\tilde{p}_d(\tau) = (p_{15}(\tau) - p_{25}(\tau))/L_{Tx}$, $\tilde{p}_d^y(\tau) = (p_y^{Tx_1}(\tau) - p_y^{Tx_2}(\tau))/L_{Tx}$ and $\tilde{p}_d^z(\tau) = (p_z^{Tx_1}(\tau) - p_z^{Tx_2}(\tau))/L_{Tx}$. Here the subscript d indicates that the transmitter is a dipole. The transmitted symbol vector is defined as $\mathbf{S} = [s_0\ s_1\ s_2\ \cdots\ s_{K-1}]^T$. The channel matrix is $\mathbf{H} = [\mathbf{H}_1^\dagger\ \mathbf{H}_2^\dagger\ \mathbf{H}_3^\dagger]^\dagger$, where † denotes the complex conjugate transpose of a matrix and

$$\mathbf{H}_l = \begin{bmatrix} h_l(0) & & \\ \vdots & \ddots & h_l(0) \\ h_l(M-1) & \ddots & \vdots \\ & & h_l(M-1) \end{bmatrix},\ l = 1,\ 2,\ 3, \quad (9)$$

where $h_1 = \tilde{p}_d$, $h_2 = \tilde{p}_d^y$ and $h_3 = \tilde{p}_d^z$. Let the noise vector be $\mathbf{N} = [\mathbf{N}_1^T\ \mathbf{N}_2^T\ \mathbf{N}_3^T]^T$, where

$$\mathbf{N}_l = [n_l(0)\ \ n_l(1)\ \ \cdots\ \ n_l(K+M-2)]^T,\ l = 1,\ 2,\ 3, \quad (10)$$

and $n_1 = n$, $n_2 = n_y$ and $n_3 = n_z$. These are the noise terms in (8). The vector of received symbols can be written as

$$\mathbf{R} = \mathbf{HS} + \mathbf{N}. \quad (11)$$

Here $\mathbf{R} = [r(0)\ \cdots\ r(K+M-2)\ r_y(0)\ \cdots\ r_y(K+M-2)\ r_z(0)\ \cdots\ r_z(K+M-2)]^T$ and r, r_y and r_z are the received pressure, y-velocity and z-velocity signals in (8).

Assuming perfect channel estimate at *Rx*, here we use a zero forcing equalizer to investigate the feasibility of symbol detection in the proposed system in Fig. 1. The minimum variance unbiased estimate of the transmitted symbol vector $\mathbf{S}$ is [9]

$$\hat{\mathbf{S}} = (\mathbf{H}^\dagger \boldsymbol{\Sigma}^{-1} \mathbf{H})^{-1} \mathbf{H}^\dagger \boldsymbol{\Sigma}^{-1} \mathbf{R}, \quad (12)$$

where $\mathbf{\Sigma} = E[\mathbf{N}\mathbf{N}^{\dagger}]$ is the covariance matrix of the noise in (11). The covariance matrix of the symbol estimation error can be written as [9]

$$\mathbf{W} = E[(\hat{\mathbf{S}} - \mathbf{S})(\hat{\mathbf{S}} - \mathbf{S})^{\dagger}] = (\mathbf{H}^{\dagger}\mathbf{\Sigma}^{-1}\mathbf{H})^{-1}. \quad (13)$$

For BPSK modulation and similarly to [10] and [11], the average bit error rate (BER) for a block of size K, after the zero forcing equalization in (12) can be written as

$$\overline{P}_e = \frac{1}{K}\sum_{i=1}^{K} Q(\sqrt{2\Omega_s / w_{ii}}). \quad (14)$$

Here Ω_s is the average symbol power, w_{ii} is the i-th diagonal element of $\mathbf{W}$ in (13), and $Q(x) = (2\pi)^{-1/2}\int_x^{+\infty}\exp(-x^2/2)dx$.

In simulations, channel impulse responses are generated using Bellhop [12] and relevant parameters are given in Table I. The sound speed profile is the one obtained during underwater communication experiments conducted in 2002, in waters off San Diego, CA [13] and shown in Fig. 2. $L_{Rx} = L_{Tx} = 0.1\lambda,\ 0.2\lambda$ and $K = 200$ BPSK symbols at a bit rate of 2400 bits/sec. are transmitted.

TABLE I
SIMULATION PARAMETERS

Water depth (m)	81.158
Water density (kg/m^3)	1024
Transmitter depth (m)	$z_0' = 25$
Transmitter take-off angle (degree)	-30 to 30
Number of beams	2001
Bottom type	Coarse silt and very fine sand
Receiver depth (m)	$z_0 = 63$
Receiver range (km)	$y_0' - y_0 = 1$
Carrier frequency (Hz)	12000
Sampling frequency (Hz)	48000
Data rate (Hz)	2400
Nominal sound speed (m/s)	1500
Wavelength (m)	0.125

To define the average signal-to-noise ratio (SNR) per channel in simulations, we first define SNRs in the three channels of the system as $\zeta_d = \Omega_d / \Omega_n$, $\zeta_d^y = \Omega_d^y / \Omega_n^y$, $\zeta_d^z = \Omega_d^z / \Omega_n^z$, where $\Omega_d = (\tilde{\mathbf{p}}_d)^{\dagger}\tilde{\mathbf{p}}_d$, $\Omega_d^y = (\tilde{\mathbf{p}}_d^y)^{\dagger}(\tilde{\mathbf{p}}_d^y)$ and $\Omega_d^z = (\tilde{\mathbf{p}}_d^z)^{\dagger}(\tilde{\mathbf{p}}_d^z)$. So, the average SNR per channel is $\overline{\zeta}_d = (\zeta_d + \zeta_d^y + \zeta_d^z)/3$.

A. Channel Responses and Parameters

The amplitude of the complex impulse responses of the three channels in (8) are shown in Fig. 3 for two different bottom types with $L_{Rx} = L_{Tx} = 0.2\lambda$. The pressure channel impulse response p from (y_0', z_0') to (y_0, z_0) , element no. 5, is shown in Fig. 3 as a reference. Average powers of the four channels in Fig. 3 are normalized to 1. The amplitude of the Fourier transforms of the impulse responses of Fig. 3 are shown in Fig. 4. The amplitude of complex correlations between each two channels of (8) are listed in Table II. Except of the correlation of 0.55, the other channel correlations are very small. This indicates a good level of diversity with compact transmit and receive vector sensors in the proposed system. RMS delay spreads [14] of channels in (8) are also provided in Table II. It appears that for very fine sand, the RMS delay spreads are smaller. Also τ_{rms} for the channel $(p_{15} - p_{25})/L_{Tx}$ appears to be larger.

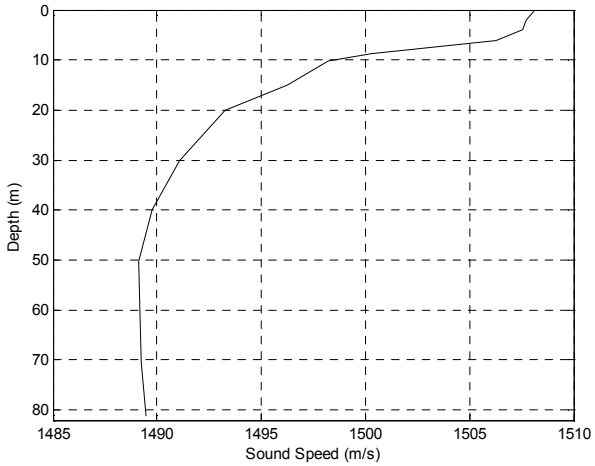

Fig. 2. Sound speed versus the water depth

TABLE II
CHANNEL CORRELATIONS AND RMS DELAY SPREADS

Bottom type	Coarse silt	Very fine sand
Correlation of $(p_{15} - p_{25})/L_{Tx}$ and $(p_y^{Tx_1} - p_y^{Tx_2})/L_{Tx}$	0.55	0.15
Correlation of $(p_{15} - p_{25})/L_{Tx}$ and $(p_z^{Tx_1} - p_z^{Tx_2})/L_{Tx}$	0.069	0.027
Correlation of $(p_y^{Tx_1} - p_y^{Tx_2})/L_{Tx}$ and $(p_z^{Tx_1} - p_z^{Tx_2})/L_{Tx}$	0.17	0.06
RMS delay spread of $(p_{15} - p_{25})/L_{Tx}$ (msec)	1.3	0.85
RMS delay spread of $(p_y^{Tx_1} - p_y^{Tx_2})/L_{Tx}$ (msec)	0.51	0.18
RMS delay spread of $(p_z^{Tx_1} - p_z^{Tx_2})/L_{Tx}$ (msec)	0.67	0.0016

B. System Performance

The BER of the proposed system is plotted in Fig. 5 using (14) for two different dipole sizes. The dipole size seems to slightly affect the performance. The key advantage of the proposed dipole transmitter is that in the reverse (reception) mode, it provides diversity. This is because it can measure both pressure and particle velocity signals.

IV. CONCLUSION

In this paper, data transmission in acoustic particle velocity channels for underwater systems is proposed and investigated in detail. Based on the derived ocean acoustical system equations and simulation analytical results, the possibility of signal modulation in particle velocity channels is demonstrated. The results provide new opportunities for underwater communication.

APPENDIX

CHARACTERIZATION OF THE ACOUSTIC CHANNELS IN THE PROPOSED SYSTEM

Consider Fig. 6, where there are two dipoles, one at the transmitter and the other at the receiver. The size of these two dipoles are L_{Tx} and L_{Rx} , respectively. Let the size of each pressure sensor in Fig. 6, the black circles, be much smaller than λ . Then the baseband acoustic pressure produced by such a

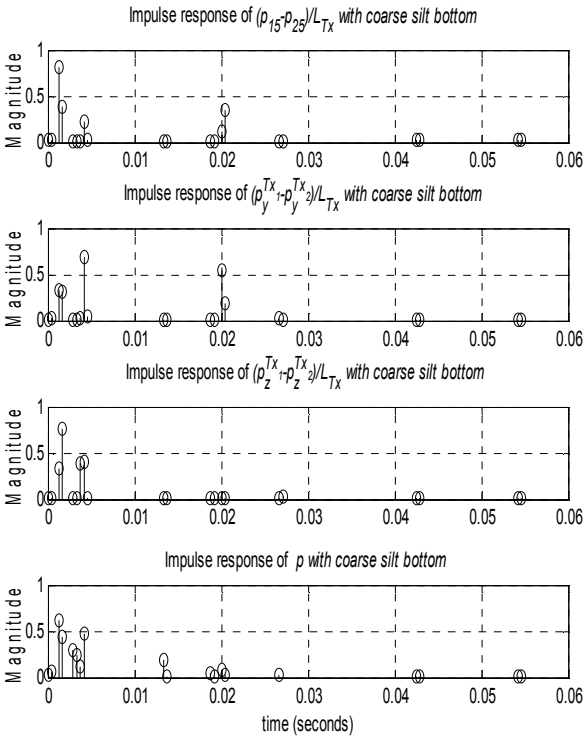

(a) Coarse silt

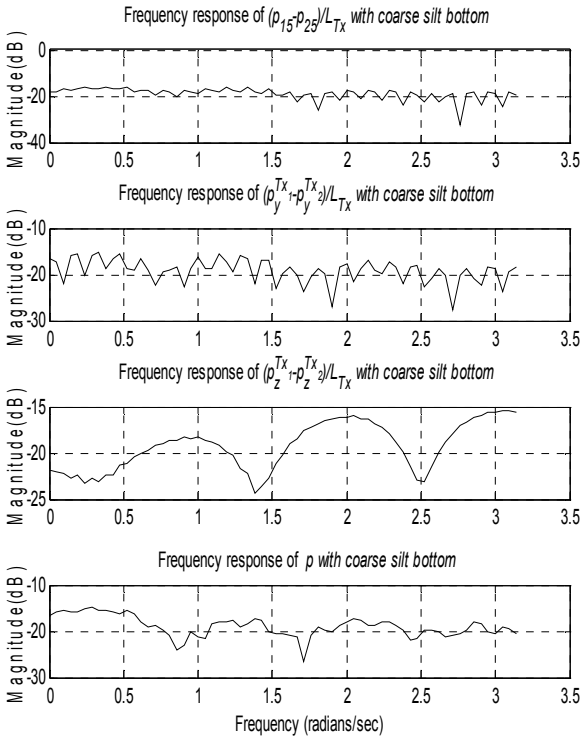

(a) Coarse silt

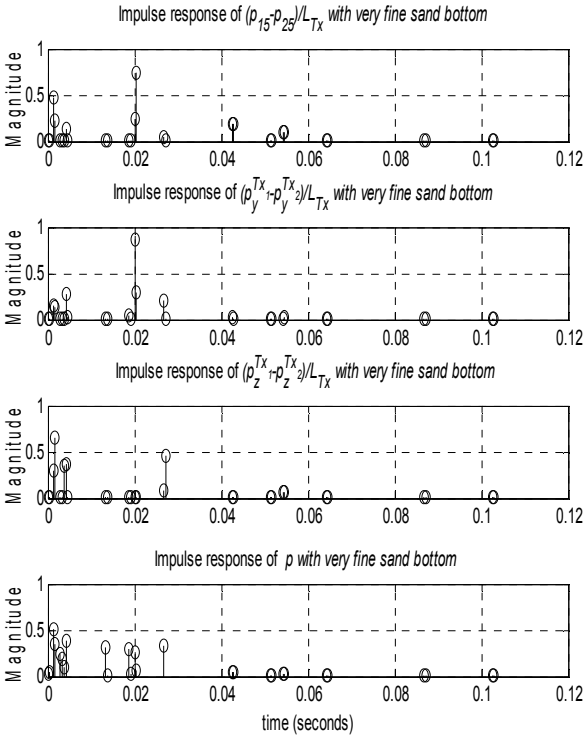

(b) Very fine sand

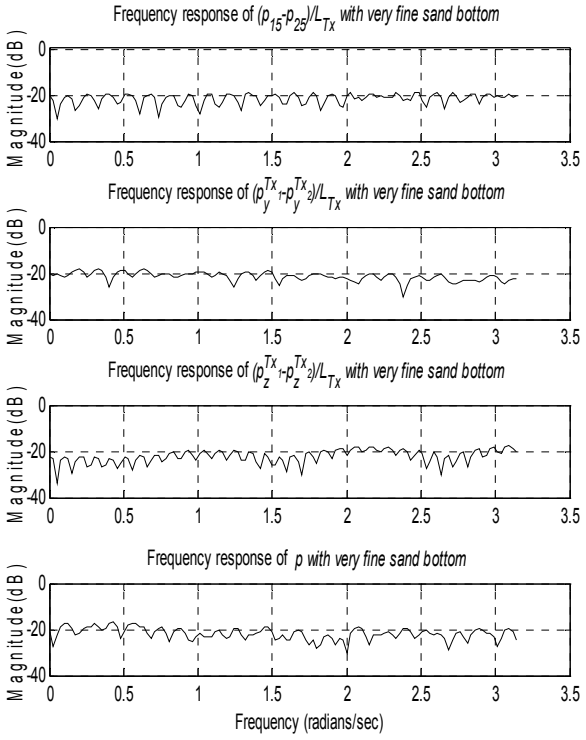

(b) Very fine sand

Fig. 3. Channel impulse responses in the proposed system operating in shallow waters with coarse silt or very fine sand sediments

Fig. 4. Channel frequency responses in the proposed system operating in shallow waters with coarse silt or very fine sand sediments

small spherical source of strength Γ_s at the point *Tx* and measured at the point *Rx* is given by [15]

$$p = (j\rho_0 ck\Gamma_s/(4\pi\ell))e^{-jk\ell}. \quad (15)$$

Here ℓ is the distance between the points *Tx* and *Rx* and $k = 2\pi/\lambda$ is the wavenumber, with λ as the wavelength. If two small spherical sources of equal strength and a 180 degree phase difference are placed at the points Tx_1 and Tx_2 as shown in Fig. 6, then the acoustic pressure produced by this dipole at the point *Rx* can be written as [15]

$$p_d = (jkL_{Tx} + (L_{Tx}/\ell))\cos\theta \times p, \quad (16)$$

where θ is the departure angle at the transmit side, as shown in Fig. 6. Eq. (16) is derived assuming $L_{Tx} \ll \ell$ and $L_{Tx} \ll \lambda$. Since for cases of interest ℓ is very large, say several kilometers, then L_{Tx}/ℓ becomes negligible in (16). This results in

$$p_d / L_{Tx} = jk\cos\theta \times p. \quad (17)$$

Since $L_{Tx} \ll \ell$, one can obtain the following expression for ℓ_2 in Fig. 6

$$\ell_2 = \sqrt{(\ell\cos\theta + (L_{Tx}/2))^2 + (\ell\sin\theta)^2} \approx \ell + (L_{Tx}\cos\theta)/2. \quad (18)$$

Using (18), (15) can be re-written as

$$p = (j\rho_0 ck\Gam_s/(4\pi\ell))e^{-jk(\ell_2 - (L_{Tx}\cos\theta)/2)}. \quad (19)$$

By taking the derivation of *p* in (19) in the *z* direction we obtain

$$\partial p/\partial(L_{Tx}/2) = (-\rho_0 ck^2\Gamma_s/(4\pi\ell))e^{-jk\ell}\cos\theta. \quad (20)$$

Using (15), this can be re-written as

$$\partial p/\partial(L_{Tx}/2) = jk\cos\theta \times p. \quad (21)$$

Comparison of (17) and (21) shows

$$p_d / L_{Tx} = \partial p/\partial(L_{Tx}/2). \quad (22)$$

This result shows that the pressure produced by a dipole upon $\Gamma_s/-\Gamma_s$ signaling is the same as the remote vertical spatial gradient of the pressure that would have been produced by a single transmitter of strength Γ_s located at the point *Tx* in Fig. 6.

Now we investigate the signals produced by the transmit dipole and measured by the receive dipole. The distance between the points *Tx* and Rx_1 in Fig. 6 can be written as

$$\ell_1' = \sqrt{(\ell\cos\theta + (L_{Rx}/2))^2 + (\ell\sin\theta)^2} \approx \ell + (L_{Rx}\cos\theta)/2. \quad (23)$$

Then using (15) and (17), the acoustic pressure produced by the dipole at the point Rx_1 is

$$p_d^{Rx_1} / L_{Tx} = (-\rho_0 ck^2\Gamma_s/(4\pi\ell_1'))e^{-jk\ell_1'}\cos\theta_1'. \quad (24)$$

For Rx_2 we similarly have

$$\ell_2' = \sqrt{(\ell\cos\theta - (L_{Rx}/2))^2 + (\ell\sin\theta)^2} \approx \ell - (L_{Rx}\cos\theta)/2, \quad (25)$$

$$p_d^{Rx_2} / L_{Tx} = (-\rho_0 ck^2\Gamma_s/(4\pi\ell_2'))e^{-jk\ell_2'}\cos\theta_2'. \quad (26)$$

Since $\ell \gg L_{Rx}$ in Fig. 6, for ℓ_1' and ℓ_2' in the denominators of (24) and (26) we have $\ell_1' \approx \ell_2' \approx \ell$ and also $\theta_1' \approx \theta_2' \approx \theta$. Therefore, the spatial gradient measured by the receive vector sensor can be written as

$$p_d^{Rx_1} / L_{Tx} - p_d^{Rx_2} / L_{Tx} = (-\rho_0 ck^2\Gamma_s/(4\pi\ell))e^{-jk\ell} \times (e^{-jkL_{Rx}\cos\theta/2} - e^{jkL_{Rx}\cos\theta/2})\cos\theta, \quad (27)$$

where ℓ_1' and ℓ_2' in the exponents are replaced by their equivalents in (23) and (25). Since $L_{Rx} \ll \ell$, we have $\cos(kL_{Rx}\cos\theta/2) \approx 1$ and $\sin(kL_{Rx}\cos\theta/2) \approx kL_{Rx}\cos\theta/2$. This simplifies (27) to

$$p_d^{Rx_1} / L_{Tx} - p_d^{Rx_2} / L_{Tx} = (j\rho_0 ck^3 L_{Rx}\Gamma_s/(4\pi\ell))e^{-jk\ell}\cos^2\theta. \quad (28)$$

Using (15), (28) can be finally written as

$$(p_d^{Rx_1} / L_{Tx} - p_d^{Rx_2} / L_{Tx}) / L_{Rx} = k^2\cos^2\theta \times p. \quad (29)$$

On the other hand, using (25), *p* in (15) can be written as

$$p = (j\rho_0 ck\Gamma_s/(4\pi\ell))e^{-jk(\ell_2' + (L_{Rx}\cos\theta)/2)}. \quad (30)$$

According to the definition of particle acceleration [16], second spatial derivation of *p* in (30) gives the particle acceleration at the point *Rx*, produced by the pressure transmitter at the point *Tx*

$$\partial^2 p/\partial(L_{Rx}/2)^2 = -k^2\cos^2\theta \times p. \quad (31)$$

Comparison of (30) and (31) results in

$$(p_d^{Rx_1} / L_{Tx} - p_d^{Rx_2} / L_{Tx}) / L_{Rx} = -\partial^2 p/\partial(L_{Rx}/2)^2. \quad (32)$$

This means the particle velocity produced by a dipole upon $\Gamma_s/-\Gamma_s$ signaling and measured by a dipole at the receiver is equivalent to the particle acceleration that would have been generated by a single transmitter of strength Γ_s located at the point *Tx* in Fig. 6.

REFERENCES

[1] *Proc. AIP Conf. Acoustic Particle Velocity Sensors: Design, Performance, and Applications*, Mystic, CT, 1995.

[2] *Proc. Workshop Directional Acoustic Sensors (CD-ROM)*, New Port, RI, 2001.

[3] A. Nehorai and E. Paldi, "Acoustic vector-sensor array processing," *IEEE Trans. Signal Processing*, vol. 42, pp. 2481-2491, 1994.

[4] J. C. Shipps and K. Deng, "A miniature vector sensor for line array applications," in *Proc. Oceans*, San Diego, CA, 2003, pp. 2367-2370.

[5] C. H. Sherman and J. L. Butler, *Transducers and Arrays for Underwater Sound*. New York: Springer, 2007.

[6] A. Abdi and H. Guo, "A new compact multichannel receiver for underwater wireless communication networks," *IEEE Trans. Wireless Commun.*, vol. 8, pp. 3326-3329, 2009.

[7] A. Abdi, H. Guo and P. Sutthiwan, "A new vector sensor receiver for underwater acoustic communication," in *Proc. Oceans*, Vancouver, BC, Canada, 2007 (10 pages).

[8] A. Abdi and H. Guo, "Signal correlation modeling in acoustic vector sensor arrays," *IEEE Trans. Signal Processing*, vol. 57, pp. 892-903, 2009.

[9] S. M. Kay, *Fundamentals of Statistical Signal Processing: Estimation Theory*. Englewood Cliffs, NJ: PTR Prentice-Hall, 1993.

[10] S. Ohno, "Performance of single-carrier block transmissions over multipath fading channels with linear equalization," *IEEE Trans. Signal Processing*, vol. 54, pp. 3678 – 3687, 2006.

[11] C. Tepedelenlioglu and Q. Ma, "On the performance of linear equalizers for block transmission systems," in *Proc. IEEE Globol Telecommun. Conf.,* St. Louis, MO, 2005, pp. 3892-3896.

[12] A. Dunkan and A. Maggi. Underwater Acoustic Propogation Modeling Software. [Online]. Available: http://cmst.curtin.edu.au/

[13] P. S. Duke, "Direct-sequence spread-spectrum modulation for utility packet transmission in underwater acoustic communication networks," M.S. thesis, Dept. Elec. Comp. Eng., Naval Postgraduate School, Monterey, CA, 2002.

[14] A. F. Molisch, *Wireless Communication*, New York: Wiley, 2005.

[15] E. Kinsler and A. R. Frey, *Fundamentals of Acoustics*, 2nd ed., New York: Wiley, 1962.

[16] B. A. Cray, V. M. Evora and A. H. Nuttall, "Highly directional acoustic receivers," *J. Acoust. Soc. Am.*, vol. 113, pp. 1526-1532, 2003.

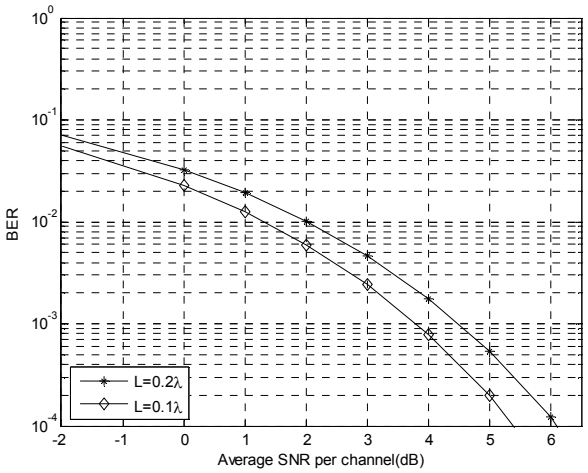

(a) Coarse silt

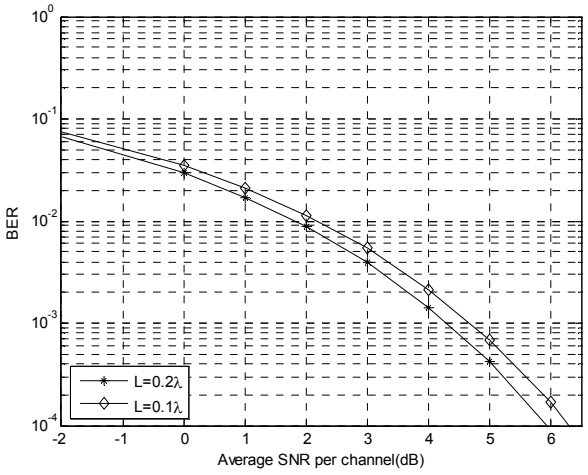

(b) Very fine sand

Fig. 5. Performance of the proposed system with $L = L_{Rx} = L_{Tx} = 0.1\lambda,\ 0.2\lambda$ and two different sediments.

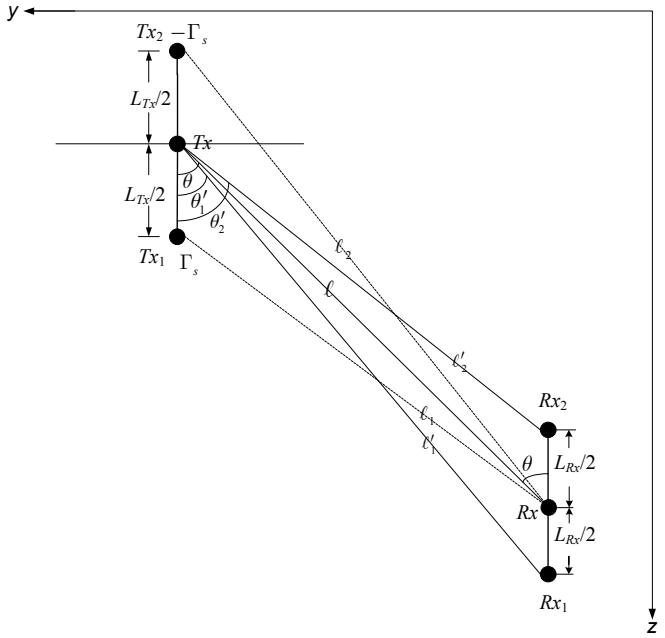

Fig. 6. Geometrical configuration of the system with one transmit dipole and one receive dipole.